Computational Studies on SO_4 and S_2O_3

Michael L. McKee

Contribution from the Department of Chemistry, Auburn University, Auburn, Alabama 36849

Received December 9, 1992

Abstract: Several structures has been considered for the neutral SO_4 species observed in a low-temperature matrix. The lowest-energy structure is predicted to have a three-membered SOO ring and C_{2v} symmetry. Vibrational frequencies at the MP2/6-31+G* level of theory and isotope shifts for this structure are in good agreement with experiment. Disulfur trioxide (S_2O_3) is predicted to have a three-membered SSO ring (rather than an SOO ring) and to be 12.7 kcal/mol more stable than SO_3 + $S(^3P)$.

Introduction

Although the chemistry of SO_4 has not been widely investigated, there is good evidence that it can be prepared. Kugel and Taube[1] generated the species by photolysis of O_3 in an Ar matrix containing SO_3 at 15 K. They obtained infrared spectra of SO_4 as a function of matrix composition, and they also reported infrared isotopic shifts for both ^{18}O and ^{34}S. Two very strong bands at 1434 and 1267 cm^{-1} were assigned to the symmetric and asymmetric stretches of an SO_2 moiety. The species is stable up to 100–150 K, but upon further warming, it undergoes a complex decomposition reaction. Schriver et al.[2] also report IR bands at 1442.9 and 1272 cm^{-1}, which they attribute to SO_4, after prolonged photolysis of a SO_3/O_3 mixture in an argon matrix.

SO_4 is potentially relevant to atmospheric chemistry, because it is produced by the reaction of $O(^3P)$ with SO_3, both of which are atmospheric constituents. Calvert et al.[3] have discussed this possibility; they concluded that the reaction could be neglected because the reaction of SO_3 with atmospheric H_2O is much faster. However, a recent study of the kinetics of reaction of SO_3 with H_2O has shown that its rate constant is more than two orders of magnitude lower than was previously believed.[4] The significance of SO_4 needs to be reevaluated.

The structure and vibrational frequencies of SO_4 are the focus of the present paper. Kugel and Taube[1] used their isotopic infrared data to assign either a C_{2v} **1** three-membered ring structure or an open C_1 **2** (or C_s **3**) structure:

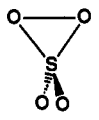

C_{2v} (1)

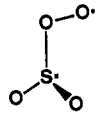

C_s (2) C_1 (3)

A tentative assignment of the SO_4 species to the C_{2v} structure (**1**) was made on the basis of vibrational frequencies of known metal dioxygen complexes. In a subsequent study, LaBonville et al.[5] performed a normal coordinate analysis and assigned the peroxysulfuryl C_s structure (**2**). This structure (but reduced in symmetry to C_1 **3**) was also supported by Anderson's ASED MO calculations.[6] In contrast to these latter reports, the present work finds that higher-level ab initio methods support the C_{2v} structure (**1**).

The two alternative structures considered for SO_4 bear some resemblance to the proposed intermediates in the oxidation of sulfides.[7,8] The possible intermediates are either a zwitterionic or biradical persulfoxide ($R_2\dot{S}O\dot{O}$) or a thiadioxirane ($R_2\overbrace{SOO}$). From the observed IR spectrum of a sulfide in an oxygen matrix at 13 K, Akasaka et al.[9] concluded that the intermediate in the oxidation was the zwitterionic species. However, evidence has also been presented[7] which suggests that formation of the thiadioxirane is competitive with formation of the zwitterionic persulfoxide. The global minimum on the R_2SO_2 surface is the sulfone,[7] which is significantly more stable than either intermediate. Of course, there is no reason to expect similar structures for R_2SO_2 and SO_4, since the sulfur in SO_4 is in a different electronic environment than in R_2SO_2.

Methods

Calculations have been made using the GAUSSIAN 90,[10] GAUSSIAN 92,[11] and GAMESS program systems.[12] Geometries were fully optimized within the appropriate point group at the HF/3-21G* and HF/6-31+G* levels, and for two structures also at the MP2/6-31+G* level.[13] Open-shell species were calculated with the unrestricted Hartree–Fock formalism. The effect of spin contamination in open-shell species has been projected out of the MP energies (PMP) by the spin-projection method developed by Schlegel and co-workers.[14] Geometry optimization at the correlated level of theory included core orbitals (FULL option) while MP4 and PMP4 calculations employed the frozen-core approximation.

Absolute energies (hartrees) are given in Table I and relative energies (kcal/mol) are given in Table II, while selected geometric parameters are given in Figure 1 for SO_4 (**1–10**), S_2O_3 (**11, 12**), and related molecules.

Vibrational frequencies have been calculated analytically at the Hartree–Fock level and by finite difference of analytical first derivatives at the MP2 level. Relative energies were not corrected for zero-point differences because several of the SO_4 stationary points yield unrealistic

(1) Kugel, R.; Taube, H. *J. Phys. Chem.* **1975**, *79*, 2130.
(2) Schriver, L.; Carrere, D.; Shriver, A.; Jaeger, K. *Chem. Phys. Lett.* **1991**, *181*, 505.
(3) Calvert, J. G.; Su, F.; Bottenheim, J. W.; Strausz, O. P. *Atmos. Environ.* **1978**, *12*, 197.
(4) Wang, X.; Jin, Y. G.; Suto, M.; Lee, L. C.; O'Neal, H. E. *J. Chem. Phys.* **1988**, *89*, 4853.
(5) LaBonville, P.; Kugel, R.; Ferraro, J. R. *J. Chem. Phys.* **1977**, *67*, 1477.
(6) Anderson, A. B. *Chem. Phys. Lett.* **1982**, *93*, 538.
(7) Watanabe, Y.; Kuriki, N.; Ishiguro, K.; Sawaki, Y. *J. Am. Chem. Soc.* **1991**, *113*, 2677.
(8) Jensen, F.; Foote, C. S. *J. Am. Chem. Soc.* **1988**, *110*, 2368.
(9) Akasaka, T.; Yabe, A.; Ando, W. *J. Am. Chem. Soc.* **1987**, *109*, 8085.
(10) GAUSSIAN 90: Frisch, M. J., Head-Gordon, M., Trucks, G. W., Foresman, J. B., Schlegel, H. B., Raghavachari, K., Robb, M., Binkley, J. S., Gonzales, C., DeFrees, D. J., Fox, D. J., Whiteside, R. A., Seeger, R., Melius, C. F., Baker, J., Martin, R. L., Kahn, L. R., Stewart, J. J. P., Topiol, S., Pople, J. A.; Gaussian, Inc.: Pittsburgh, PA, 1990.
(11) GAUSSIAN 92: Frisch, M. J. Trucks, G. W., Head-Gordon, M., Gill, P. M. W., Wong, M. W., Foresman, J. B., Johnson, B. G., Schlegel, H. B., Robb, M. A., Replogle, E. S., Gomperts, R., Andres, J. L., Raghavachari, K., Binkley, J. S., Gonzales, C., Martin, R. L., Fox, D. J., DeFrees, D. J., Baker, J., Stewart, J. J. P., Pople, J. A.; Gaussian, Inc.: Pittsburgh, PA, 1992.
(12) Schmidt, M. W.; Baldridge, K. K.; Boatz, J. A.; Jensen, J. H.; Koseki, S.; Gorden, M. S.; Nguyen, K. A.; Windus, T. L.; Elbert, S. T. GAMESS. *QCPE Bull.* **1990**, *10*, 52.
(13) For a description of basis sets see: Hehre, W. J.; Radom, L.; Schleyer, P. v. R.; Pople, J. A. *Ab Initio Molecular Orbital Theory*; Wiley: New York, 1986.
(14) Sosa, C.; Schlegel, H. B. *Int. J. Quantum Chem.* **1986**, *29*, 1001. Schlegel, H. B. *J. Chem. Phys.* **1986**, *84*, 4530.

0002-7863/93/1515-9136$04.00/0

Table I. Absolute Energies (hartrees) for Various Species at Optimized 3-21G*, 6-31+G*, and MP2/6-31+G* Geometries

			//3-21G*				//6-31+G*			
	sym	state	HF/3-21G*	HF/6-31G*	PMP2/6-31G*	PMP4/6-31G*	HF/6-31+G*	PMP2/6-31+G*	PMP4/6-31+G*	$\langle S^2\rangle$
O	K	^{1}D	−74.35056	−74.74628	−74.80425	−74.82142	−74.74887	−74.80960	−74.82736	1.01
O	K	^{3}P	−74.39366	−74.78393	−74.88131	−74.89662	−74.78676	−74.88687	−74.90274	2.01
S	K	^{1}D	−395.61094	−397.45552	−397.50754	−397.52653	−397.45621	−397.50903	−397.52816	1.02
S	K	^{3}P	−395.63122	−397.47596	−397.55420	−397.57181	−397.47669	−397.55574	−397.57348	2.01
O_2	$D_{\infty h}$	$^1\Delta_g$	−148.73864	−149.57919	−149.91716	−149.93238	−149.59294	−149.91527	−149.93256	2.04
O_2	$D_{\infty h}$	$^3\Sigma_g^-$	−148.76908	−149.60841	−149.95558	−149.96717	−149.62207	−149.95568	−149.96938	1.02
SO	$C_{\infty h}$	$^1\Delta$	−470.05394	−472.30771	−472.58676	−472.60961	−472.31357	−472.59483	−472.61860	1.03
SO	$C_{\infty h}$	$^3\Sigma$	−470.07466	−472.32734	−472.61637	−472.63610	−472.33312	−472.62449	−472.64510	2.04
SO_2	C_{2v}	$^1A_1$	−544.50373	−547.16892	−547.67442	−547.70048	−547.17570	−547.68810	−547.71535	
S_2O	C_s	$^1A'$	−865.70915	−869.80662	−870.25703	−870.29514	−869.81310	−870.27002	−870.30905	
SO_3	D_{3h}	$^1A_1'$	−618.91501	−621.98140	−622.66322	−622.69050	−621.98846	−622.67845	−622.70751	
SO_4 **1**	C_{2v}	$^1A_1$	−693.25472	−696.70327	−697.57985	−697.61648	−696.71256	−697.59235	−697.63078	
O_2SOO **2**	C_s	$^1A''$	−693.23969	−696.68849	−697.51602	−697.56700	−696.70643	−697.54221	−697.59378	1.04
O_2SOO **3**	C_1	^1A	no minimum				−696.71201	−697.55069	−697.60202	1.03
SO_4 (l) **4**	C_{3v}	^1E	−693.28414	−696.73008	−697.54014	−697.59293	−696.73834	−697.56099	−697.61707	1.09
SO_4 (s) **5**	C_{3v}	^1E	−693.27716	−696.72488	−697.53370	−697.58612	−696.73325	−697.55428	−697.60979	1.07
SO_4 **6**	C_{3v}	$^1A_1$	−693.14444	−696.58955	−697.54919	−697.58124	−696.59753	−697.57009	−697.60548	
SO_4 **7**	C_{3v}	^3E	−693.29107	−696.73706	−697.52794	−697.58107	−696.74552	−697.54914	−697.60533	2.05
SO_4 **8**	C_{3v}	$^3A_2$	−693.29218	−696.73503	−697.53956	−697.58856	−696.74392	−697.55988	−697.61199	2.13
SO_4 **9**	C_s	$^1A''$	−693.29662	−696.74504	−697.55231	−697.60244	−696.75281	−697.57299	−697.62609	1.06
SO_4 **10**	C_s	$^3A''$	−693.29890	−696.74601	−697.54253	−697.59336	−696.75411	−697.56748	−697.61726	2.07
O_2SSO **11**	C_s	$^1A'$	−1014.51670	−1019.41974	−1020.23149	−1020.27701	−1019.42996	−1020.25322	−1020.30117	
$SOSOO$ **12**	C_s	$^1A'$	−1014.45100	−1019.33810	−1020.16387	−1020.21178	−1019.34956	−1020.17841	−1020.22810	

			//MP2/6-31+G*			
			HF/6-31+G*	PMP2/6-31+G*	PMP4/6-31+G*	$\langle S^2\rangle$
SO_4	C_{2v}	$^1A_1$	−696.69392	−697.60937	−697.65110	
SO_4	C_s	$^1A''$	−696.74659	−697.57959	−697.63431	1.06

Table II. Relative Energies (kcal/mol) for Various Species at Optimized 3-21G*, 6-31+G*, and MP2/6-31+G* Geometries

			//3-21G*				//6-31+G*			//MP2/6-31+G*		
	sym	state	HF/ 3-21G*	HF/ 6-31G*	PMP2/ 6-31G*	PMP4/ 6-31G*	HF/ 6-31+G*	PMP2/ 6-31+G*	PMP4/ 6-31+G*	HF/ 6-31+G*	PMP2/ 6-31+G*	PMP4/ 6-31+G*
$O + SO_3$	K, D_{3h}	$^1D, ^1A_1'$	−6.8	−15.3	70.5	65.6	−15.5	65.4	60.2			
$O + SO_3$	K, D_{3h}	$^3P, ^1A_1'$	−25.9	−33.6	46.4	43.8	−33.8	40.0	37.1			
$SO_2 + O_2$	$C_{2v}, D_{\infty h}$	$^1A_1, ^1\Delta_g$	7.7	−28.1	−7.4	−10.3	−35.2	−6.9	−10.7			
SO_4 **1**	C_{2v}	$^1A_1$	0.0	0.0	0.0	0.0	0.0	0.0	0.0	0.0	0.0	0.0
O_2SOO **2**	C_s	$^1A''$	9.4	9.3	40.0	31.0	3.8	31.5	23.2			
O_2SOO **3**	C_1	^1A	no minimum				0.3	26.1	18.0			
SO_4 (l) **4**	C_{3v}	^1E	−18.5	−16.8	24.9	14.8	−16.2	19.7	8.6			
SO_4 (s) **5**	C_{3v}	^1E	−14.1	−13.6	29.0	19.0	−13.0	23.9	13.2			
SO_4 **6**	C_{3v}	$^1A_1$	69.2	71.4	19.2	22.1	72.2	14.0	15.9			
SO_4 **7**	C_{3v}	^3E	−22.8	−21.2	32.6	22.2	−20.7	27.1	16.0			
SO_4 **8**	C_{3v}	$^3A_2$	−23.5	−19.9	25.3	17.5	−19.7	20.4	11.8			
SO_4 **9**	C_s	$^1A''$	−26.3	−26.2	17.3	8.8	−25.2	12.1	2.9	−33.0	18.7	10.5
SO_4 **10**	C_s	$^3A''$	−27.7	−26.8	23.4	14.5	−26.1	15.6	8.5			
$S + SO_3$	K, D_{3h}	$^1D, ^1A_1'$	−5.8	−10.8	38.1	37.6	−9.2	41.2	41.1			
$S + SO_3$	K, D_{3h}	$^3P, ^1A_1'$	−18.5	−23.6	8.8	9.2	−22.0	11.9	12.7			
$SO_2 + SO$	$C_{2v}, C_{\infty v}$	$^1A_1, ^1\Delta$	−25.7	−35.7	−18.6	−20.8	−37.2	−18.6	−20.6			
$S_2O + O_2$	$C_s, D_{\infty h}$	$^1A', ^1\Delta_g$	43.2	21.3	36.0	31.0	15.0	42.6	37.4			
O_2SSO **11**	C_s	$^1A'$	0.0	0.0	0.0	0.0	0.0	0.0	0.0			
$SOSOO$ **12**	C_s	$^1A'$	41.2	51.2	42.4	40.9	50.4	46.9	45.8			

frequencies. The problem is revealed by frequencies (real or imaginary) that are too large (i.e. >6000 cm^{-1}). A similar situation has been found for analytical frequencies of the Hartree–Fock wave function of twisted ethylene where an imaginary frequency of 10138i was reported with a standard DZ basis set.[15] The result is an indication that standard single-configurational methods may not be adequate for describing the electronic wave function in these systems. However, it should be pointed out a single-configurational method supplemented by perturbative correlations for electron correlation was found to be very close in energy to a large MCSCF treatment near a crossing point in the H_4^+ system,[16] a section of the potential energy surface where single-configurational methods are often cited as being unreliable. While other properties (e.g. frequencies, charge distributions, etc.) may quickly become unreliable due to the symmetry-breaking phenomena, relative energy (based on a single-configurational method and corrected by perturbation theory) may be somewhat more accurate. The Hartree–Fock and MP2 frequencies of **1** did not suffer from the above-mentioned difficulties, which is no doubt due to the fact that the wave function for this structure is better described by a single (HF) configuration.

Results and Discussion

The electron configuration of sulfur tetraoxide in T_d symmetry gives rise to degenerate electronic states, which are Jahn–Teller unstable[17] and distort to lower-symmetry and lower-energy

(15) Yamaguchi, Y.; Osamura, Y.; Schaefer, H. F. *J. Am. Chem. Soc.* **1983**, *105*, 7506.
(16) Jungwirth, P.; Čársky, P.; Bally, T. *Chem. Phys. Lett.* **1992**, *195*, 371.
(17) Jahn, H. A.; Teller, E. *Proc. R. Soc. London, Ser. A* **1937**, *A161*, 220.

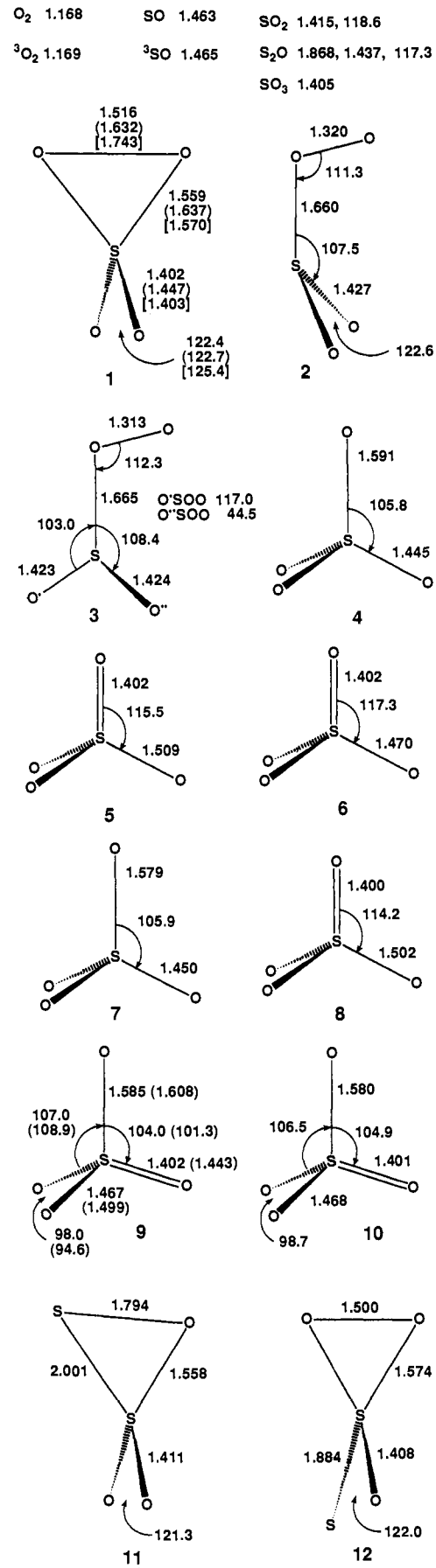

Figure 1. Selected geometric parameters (in ångströms and degrees) are given at the (U)HF/6-31+G* level for SO_4 species **1–10**, for S_2O_3 species **11** and **12**, and for miscellaneous species (O_2, SO, SO_2, S_2O, and SO_3). Values in parentheses are at the (U)MP2/6-31+G*) level and those in brackets are at the CAS(2×2)/6-31G* level.

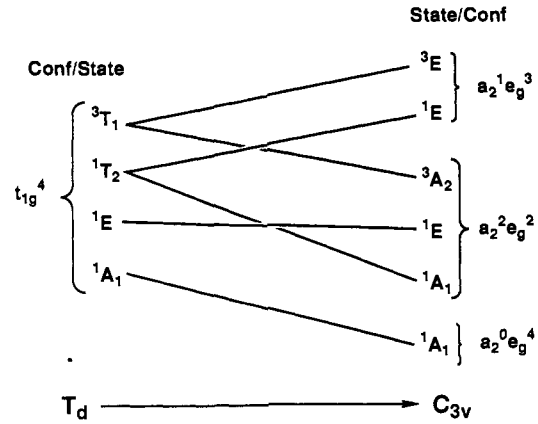

Figure 2. Schematic depiction of the electronic states involved in the descent in symmetry from T_d to C_{3v}.

structures. To determine the nature of these structures it is instructive to consider the analogous systems, CH_4^+ and CH_4^{2+}. Like SO_4^{2-}, CH_4 has tetrahedral symmetry. The HOMO of both species is triply degenerate: t_1 symmetry for SO_4^{2-} and t_2 for CH_4.

One way of determining the preferred direction of distortion is the epikernel principle[18,19] which states that the distortion is toward the "maximal allowed subgroup of the undistorted parent group". Wang and Boyd[20] have investigated the epikernel principle for the BH_3^+ radical in relation to the electron distribution of the HOMO. One component of the canonical HOMO in D_{3h} symmetry (e_1 symmetry) transforms under the C_{2v} subgroup and a distortion of the nuclei toward C_{2v} symmetry would make the average electron–nuclear distance shorter and lead to a lower energy. Their discussion considers only the first-order Jahn–Teller effect and they state that in other systems the coupling between the ground state and excited states (second-order Jahn–Teller effect) must be considered.

For CH_4^+, distortion is preferred along a direction which reduces the symmetry of the HOMO to one-dimensional representations, i.e. C_{2v}. This is supported by detailed quantum mechanical calculations[21–23] and confirmed by ESR experiments.[21a] However, for CH_4^{2+} the distortion required to reach the lowest-energy structure is more complicated. Theoretical calculations by Wong and Radom[24] indicate that CH_4^{2+} has a planar carbon of C_{2v} symmetry which is about 13 kcal/mol more stable than a planar structure of D_{4h} symmetry. The latter structure can be reached from T_d symmetry through a D_{2d} distortion (i.e. flattening a tetrahedron). Thus, the lowest-energy structure which results from Jahn–Teller distortions is not at all obvious.

As is indicated in Table I, SO_4 was investigated in a variety of symmetries and configurations. Figure 2 shows in a schematic way how these states arise.[25] Consider first the tetrahedral SO_4^{2-} molecule, which has a filled set of triply degenerate HOMOs. If this molecule is then ionized to give neutral tetrahedral SO_4, the remaining four valence electrons can be distributed among the HOMOs to give four electronic states: $^3T_1$, $^1T_2$, ^1E, and $^1A_1$. Descent to C_{3v} symmetry breaks the degeneracy of the two T states and leads to two pairs of states ($^3A_2$ and ^3E) and ($^1A_1$ and

(18) Ceulemans, A.; Beyens, D.; Vanquickenborne, L. G. *J. Am. Chem. Soc.* **1984**, *106*, 5824.
(19) Ceulemans, A.; Vanquickenborne, L. G. *Struct. Bonding* **1989**, *71*, 125.
(20) Wang, J.; Boyd, R. J. *J. Chem. Phys.* **1992**, *96*, 1232.
(21) (a) Knight, L. B., Jr.; Steadman, J.; Feller, D.; Davidson, E. R. *J. Am. Chem. Soc.* **1984**, *106*, 3700. (b) Frey, R. F.; Davidson, E. R. *J. Chem. Phys.* **1988**, *88*, 1775. (c) Paddon-Row, M. N.; Fox, D. J.; Pople, J. A.; Houk, K. N.; Pratt, D. W. *J. Am. Chem. Soc.* **1985**, *107*, 7696.
(22) Frey, R. F.; Davidson, E. R. *J. Chem. Phys.* **1988**, *88*, 1775.
(23) Boyd, R. J.; Darvesh, K. V.; Fricker, P. D. *J. Chem. Phys.* **1991**, *94*, 8083.
(24) Wong, M. W.; Radom, L. *J. Am. Chem. Soc.* **1989**, *111*, 1155.
(25) See: Cotton, F. A. *Chemical Application of Group Theory*; Wiley-Interscience: New York, 1971.

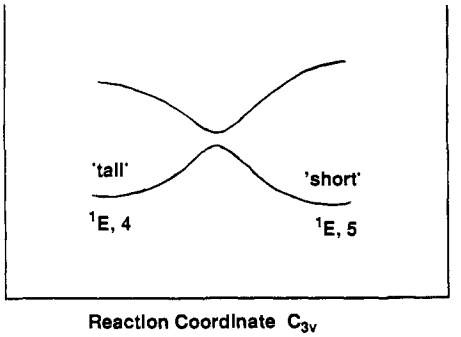

Figure 3. Reaction profile under C_{3v} constraint. The two ^{1}E states (**4**, **5**) are separated by an avoided crossing.

^{1}E). The E states are Jahn–Teller unstable, and under C_s symmetry they distort to give four states: ^{1}A′, ^{1}A″, ^{3}A′, and ^{3}A″. The C_s ^{1}A′ state is essentially a diradical, with the two unpaired electrons residing in oxygen P orbitals that are coplanar; this state is therefore unstable with respect to forming a bond between these two oxygen atoms, and this leads to a ^{1}A$_1$ state in C_{2v} symmetry. The complete roster of potential ground states thus comprises the ^{1}A$_1$ symmetry state in the C_{2v} point group (**1**), the ^{1}A″ (**9**), ^{3}A′, and ^{3}A″ (**10**) states in the C_s point group, and the ^{1}A$_1$ (**6**) and ^{3}A$_2$ (**8**) states in the C_{3v} point group.

Of these six species (where species refers to a specific state/structure combination), the ^{3}A′ C_s species is related to the ^{1}A$_1$ C_{2v} species (**1**) simply by inverting one of the electrons in the O–O bond. This should be energetically unfavorable, and therefore this ^{3}A′ species is excluded from consideration.

As is shown in Table I and II, the above five species (**1**, **6**, **8**, **9**, **10**), two peroxy species (**2**, **3**), and three species with a degenerate state of C_{3v} symmetry (**4**, **5**, **7**) have been examined at various levels of theory. An important feature of these results is that **1** is much higher in energy when the Hartree–Fock method is used, but it becomes lowest in energy when electron correlation is introduced through the Møller–Plesset method. The effect is by no means subtle, being greater than 30 kcal/mol in some cases.

The multiconfigurational character of **1** was investigated by performing a MCSCF calculation. Preliminary calculations indicated that the second most important contributor to the MCSCF wave function was the σ^* O–O orbital which would become a lone pair in the SO_4^{2-} anion. An optimization of SO_4 was carried out with a complete active space (and the 6-31G* basis set) including the occupied σ O–O orbital and the unoccupied σ^* orbitals (CAS(2×2)). The SCF configuration contributed 89% to the wave function. The σ O–O orbital has a natural population of 1.78 electrons while the σ^* O–O orbital has a natural population of 0.22 electron. While the multiconfigurational nature of the C_{2v} structure of SO_4 is significant, the SCF configuration is sufficiently dominant that electron correlation can be estimated by perturbative corrections.

When the symmetry of SO_4 is lowered from T_d to C_{3v} the symmetry of the HOMO is lowered from t_1^4 to $(a_2e_1)^4$ which gives rise to two ^{1}E states (**4**, **5**). In one ^{1}E state the $a_2^1e_1^3$ configuration is dominant while in the other ^{1}E state the $a_2^2e_1^2$ configuration is dominant. In the SCF optimization, a very different minimum was obtained depending on whether the $a_2^1e_1^3$ or $a_2^2e_1^2$ configuration was occupied. The former configuration gave a structure with a long unique S–O bond (1.591 Å), denoted the "long bond isomer" (**4**), and the latter configuration gave a structure with a short unique S–O bond (1.402 Å), denoted the "short bond isomer" (**5**).

The region around each minimum is dominated by the SCF configuration with the other configuration describing the excited state. A state crossing will occur on the reaction coordinate connecting the two stationary points in C_{3v} symmetry and an MCSCF wave function would be necessary to describe the connecting path (Figure 3). However, both ^{1}E states will Jahn–Teller distort to give (in C_s symmetry) a ^{1}A′ state and a ^{1}A″ state (**9**). The ^{1}A′ component of each ^{1}E state corresponds to a biradical which collapses to **1**. The ^{1}A″ component of both ^{1}E states leads to a common biradical (**9**), one with the α unpaired electron on one of the oxygens in the molecular plane and the β electron distributed between the two oxygens out of the molecular plane. Figure 4 illustrates the symmetry lowering and the common biradical.

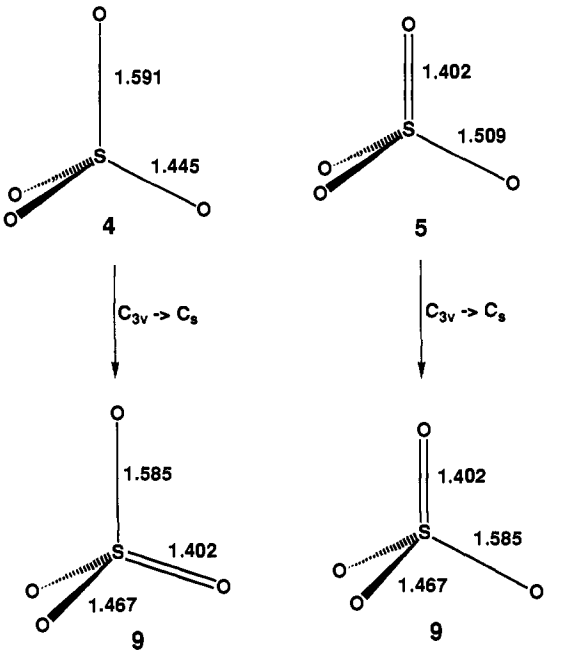

Figure 4. The ^{1}A″ components of both ^{1}E states relax to the same geometry in C_s symmetry.

At the PMP4/6-31+G* level the five states of C_{3v} symmetry (**4**–**9**) are all close in energy (8.6–16.0 kcal/mol, Table II), which is in sharp contrast to the Hartree–Fock level where the difference is almost 100 kcal/mol. With the exception of the ^{1}A$_1$ state (**6**), the *average* S–O distances in the states of C_{3v} symmetry are within 0.006 Å of each other.

In C_s symmetry, two A″ states are calculated, the singlet (**9**) and triplet (**10**) states. The singlet state (^{1}A″, **9**) is 2.9 kcal/mol less stable than **1** while the triplet state (^{3}A″, **10**) is 8.5 kcal/mol less stable than **1**. Since the energy separation between **1** and **9** is very small, the geometries of both species were reoptimized at the MP2/6-31+G* level of theory. Electron correlation stabilizes the three-membered ring, and at the MP4/6-31+G*//MP2/6-31G+G* level of theory **9** is 10.5 kcal/mol less stable than **1** (Table II).

Vibrational Frequencies

Vibrational frequencies were calculated for all species. However, as indicated above, the solution of the CPHF equations gave spurious results due to the presence of low-lying broken symmetry solutions to the SCF wave function. The stability of the wave function for the C_{2v} structure (**1**) was tested and found to be stable to release of all constraints except RHF → UHF. Thus, the onset of the symmetry-breaking phenomena was delayed sufficiently for **1** that the CPHF solution gave reasonable results at all levels including the MP2/6-31+G* level of theory.

The vibrational frequencies of SO_2 and SO_3, calculated at the HF/6-31+G* level (SO_2, 590, 1351, 1550 cm^{-1}; SO_3, 559, 581, 1209, 1540 cm^{-1}), are in reasonable agreement with experiment[26] (SO_2, 518, 1151, 1362 cm^{-1}; SO_3, 495, 529, 1068, 1391 cm^{-1}). Since frequencies of SO_2 and SO_3 have been reported at higher

Table III. Calculated Vibrational Frequencies (cm^{-1}) and IR Intensities (km) for SO_4 C_{2v} (1)

sym	HF/ 3-21G*	MP2/ 3-21G*	HF/ 6-31+G*	MP2/ 6-31+G*	exptl[a]	description
b_1	1579(309)	1487(173)	1557(347)	1436(225)	1434 (vs)	SO_2 as stretch
a_1	1414(268)	1272(137)	1402(311)	1245(186)	1267 (vs)	SO_2 s stretch
a_1	1130(3)	917(8)	1115(14)	876(30)	927	OO ring stretch
b_2	755(0)	860(91)	805(10)	795(84)	777	SO_2 as ring stretch
a_1	783(91)	652(75)	789(72)	643(66)	611	SO_2 s ring stretch
b_2	542(58)	461(30)	555(57)	455(27)	(530)	bend
a_1	540(25)	472(8)	538(27)	460(12)	498	SO_2 scissor
b_1	535(52)	466(30)	528(44)	450(27)	490	bend
a_2	379(0)	313(0)	361(0)	283(0)		twist

[a] Reference 1. The two frequncies were described as very strong (vs).

levels of theory,[26] the present objective is only to demonstrate that the HF/6-31+G* level gives reasonable agreement with experiment for the well-known SO_2 and SO_3 molecules.

A comparison is made in Table III with the vibrational frequencies calculated at the HF and MP2 levels for **1** with the 3-21G* and 6-31+G* basis sets and the experimental frequencies of the species found in the O_3/SO_3 photoirradiated matrix. The HF frequencies do not change significantly between the 3-21G* and 6-31+G* basis sets. The exception is the SO_2 asymmetric ring stretch which increases 50 cm^{-1} at the HF/6-31+G* level. The effect of electron correlation is much more pronounced. For both basis sets, the largest change HF → MP2 occurs in the O–O ring stretch which decreases 213 (3-21G*) or 239 cm^{-1} (6-31+G*). While intensities vary considerably among the different levels of theory,[27] all methods predict the symmetric and asymmetric SO_2 stretch to be the most intense. It is noteworthy that only these two bands were described as very strong in the experimental spectrum.[1]

At the highest level of theory (MP2/6-31+G*), agreement between calculation and experiment is quite good. The largest deviation is for the OO ring stretch which is underestimated by 51 cm^{-1}. The underestimation is unusual because calculated frequencies at the correlated level of theory are usually overestimated by about 5%.[28] The same mode is overestimated by 188 cm^{-1} at the HF/6-31+G* level of theory. At the Hartree–Fock level, there is no contribution from the σ(O–O) → σ^*(O–O) configuration which should make the calculated frequency for this mode too high. It appears that the contribution of the σ-(O–O) → σ^*(O–O) configuration to the OO ring stretch may be exaggerated at the MP2 level. The importance of this configuration can be seen in the O–O distance, which increases 0.116 Å on going from the HF to the MP2 level (1.516 → 1.632 Å). While vibrational frequencies were not calculated at the CAS/(2×2)/6-31G* level, it is interesting to point out that the O–O distance at that level is longer than the HF or MP2 value (1.743 Å).

The calculated isotopic shifts of the IR frequencies are presented in Table IV for the SO_4 molecule (**1**) labeled with one ^{34}S atom and with four ^{18}O atoms. With one exception, the calculated and experimental shifts are in very good agreement. The exception is the $S^{18}O_4$ shift for a bend of b_1 symmetry which is in error by 12 cm^{-1} at the MP2/6-31+G* level. The calculated isotope shift (Table IV) data taken together with the good agreement in the calculated vibrational frequencies (Table III) make a convincing argument for the C_{2v} symmetry structure as the species observed in the low-temperature matrix.[29] Calculated vibrational frequencies and isotopic shifts (UHF/6-31+G*) for the peroxy structure **3** are compared with experiment in Table V. The agreement is much poorer. The SO_2 symmetry stretch is predicted to be of only medium intensity while the experimental mode has very strong intensity. Also, the $S^{18}O_4$ isotopic shifts of the SO_2 symmetric stretch and the OO stretch are calculated to be much larger than observed.

Atomic Overlap Matrix (AOM). A method has been described by Bader[30] for determining atomic charges that are less dependent on a chosen basis set. First, critical points in electron density are located, and then a surface of zero flux is determined around each attractor (nuclear center) and the volume is integrated. These charges can be rigorously interpreted and have been found to be useful in a variety of contexts.[31] Next, the orbitals are localized by a method described by Cioslowski and the atomic overlap matrix (AOM) is determined,[32,33] the off-diagonal elements of which are the bond orders.

The AOM bond orders and the percent ionicity (0% = 100% covalent bond) are given in Table VI for the C_{2v} structure of SO_4 (**1**) calculated with the HF/3-21G* and MP2/6-31+G* methods. Several observations can be made. First, the picture does not substantially change between the HF/3-21G* and MP2/6-31+G* levels. At the higher level of theory (MP2/6-31+G*), the lone pairs on the terminal oxygens are predicted to have a bonding component with sulfur as judged by a very polar π bond. At the lower level (HF/3-21G*) the minimum contribution is not met and the electrons are described only as a lone pair. Second, despite the very long O–O bond length (1.516 Å, MP2/6-31+G*), the bond has multiple bond character (bond order = 1.12 at MP2/6-31+G*). However, the bond order does not necessarily indicate bond strength, and the σ and π components of the O–O bond may both be weak. Third, the bonding of the two terminal oxygens in SO_4 is very similar to the S–O bonding in SO_3 as judged by calculations carried out at a similar level of theory[34] (MP2/6-311+G*). Thus, the O_2 unit in SO_4 binds to SO_2 in a similar fashion as an oxygen atom in SO_3 binds to SO_2. The terminal S–O bond orders in SO_4 are 1.22 (MP2/6-31+G*) compared to values of 1.13 in SO_3 (MP2/6-311+G*). The comparison can be carried to the asymmetric SO_2 stretch in SO_4 and SO_3 (the symmetric stretch of SO_3 would involve all three oxygen atoms and would not be an appropriate comparison). At the HF/6-31+G* level, the asymmetry SO_2 stretch in SO_4 (1557 cm^{-1}) is very close to the asymmetry S–O stretch in SO_3 (1540 cm^{-1}).

An illustration of the interaction of the SO_2 fragment with O_2 in SO_4 and O in SO_3 is presented in Figure 5. In SO_4 the π bond of O_2 donates charge into the empty σ acceptor orbital of SO_2 and the lone pair of SO_2 donates charge into the empty π^* orbital of O_2. In SO_3 filled and empty p orbitals on oxygen play the role of π and π^* orbitals.

Possible Decomposition Mechanism of SO_4. The SO_4 species is stable up to 100–150 K.[1] Upon further warming, "the vacuum inside the cell degenerated and the characteristic ESR spectrum of O_2 gas was observed, indicating thermal decomposition of SO_4".[1] It may be of interest to speculate on the mechanism of decomposition. While the peroxy species (**3**) may not be the species observed in a low-temperature matrix, it may be on the pathway for decomposition of SO_4 as indicated in Figure 6. The biradical (**3**) is 18.0 kcal/mol higher in energy than the C_{2v} species

(26) See: Flament, J. P.; Rougeau, N.; Tadjeddine, M. *Chem. Phys.* **1992**, *167*, 53.
(27) Miller, M. D.; Jensen, F.; Chapman, O. L.; Houk, K. N. *J. Phys. Chem.* **1989**, *93*, 4495.
(28) DeFrees, D. J.; McLean, A. D. *J. Chem. Phys.* **1985**, *82*, 333.
(29) For a discussion of the application of calculated spectra to the identification of unusual molecules see: Hess, B. A., Jr.; Schaad, L. J. *Chem. Rev.* **1986**, *86*, 709.
(30) Bader, R. F. W. *Atoms in Molecules: A Quantum Theory*; Claredon Press: Oxford, 1990.
(31) Bader, R. F. W.; Laidig, K. E. *THEOCHEM* **1992**, *261*, 1.
(32) Cioslowski, J.; Mixon, S. T. *J. Am. Chem. Soc.* **1991**, *113*, 4142.
(33) Cioslowski, J.; Surján, P. R. *THEOCHEM* **1992**, *255*, 9.
(34) Cioslowski, J.; Mixon, S. T. Private communication.
(35) Chase, M. W., Jr.; Davies, C. A.; Downey, J. R., Jr.; Frurip, D. J.; McDonald, R. A.; Syverud, A. N. *J. Phys. Chem. Ref. Data* **1985**, *14*, Suppl. 1; *JANAF Thermochemical Tables*, 3rd ed.

Table IV. Calculated Isotope Shifts (cm^{-1}) for SO_4 C_{2v} (**1**)

	$^{32}S^{18}O_4$					$^{34}S^{16}O_4$				
sym	HF/3-21G*	MP2/3-21G*	HF/6-31+G*	MP2/6-31+G*	obs	HF/3-21G*	MP2/3-21G*	HF/6-31+G*	MP2/6-31+G*	obs
b_1	48	45	48	44	47	21	20	21	19	16
a_1	49	48	48	47	44	16	12	16	12	11
a_1	64	50	62	46	44	1	1	2	2	1
b_2	35	31	36	29	31	3	9	5	8	10
a_1	35	28	37	30	29	5	5	4	5	1
b_2	17	19	18	18		3	4	8	4	
a_1	30	26	29	25		6	0	1	0	
b_1	25	22	25	21	9	3	2	4	3	3
a_2	22	18	21	16		0	0	0	0	

Table V. Calculated Vibrational Frequencies (cm^{-1}), IR Intensities (km), and Isotope Shifts (cm^{-1}) of O_2SOO (**3**) at the UHF/6-31+G* Level

		isotope shifts				
		$^{32}S^{18}O_4$		$^{34}S^{16}O_4$		
freq (int)	exptl[a,b]	calc	exptl	calc	exptl	description
1410 (130)	1434 (vs)	44	47	18	16	SO_2 as stretch
1209 (39)	1267 (vs)	57	44	5	11	SO_2 s stretch
1184 (81)	927	65	44	1	1	OO stretch
766 (135)	777	30	31	7	10	SO stretch
555 (41)	*611*	*18*	*29*	*7*	*1*	*SO_2 wag*
525 (35)	(530)	21		5		SOO bend
427 (9)	490	23	9	1	3	SO_2 scissor
283 (3)	498	15		1		SO_2 rock
118 (1)		6		0		torsion

[a] Reference 1. The two frequencies were described as very strong (vs). [b] The present work suggests that the experimental frequencies refer to the C_{2v} structure **1** rather than the peroxy structure **3**.

Table VI. AOM-Based Covalent Bond Orders and Percent Ionicity for SO_4 C_{2v} (**1**) and SO_3

	SO_4				SO_3	
	HF/3-21G*		MP2/6-31+G*		MP2/6-311+G* [a]	
	AOM	ionicity[b]	AOM	ionicity[b]	AOM	ionicity[b]
S_1O_2	0.76	σ 56.2	0.71	σ 61.2		
O_2O_3	1.22	σ 0.0	1.12	σ 0.0		
S_1O_4	1.31	σ 41.1	1.22	σ 58.3	1.13	σ 54.7
				π 78.0		π 70.0
O_4O_2	0.14		0.14			
O_4O_5	0.22		0.22		0.25	

[a] Reference 34. [b] Percent.

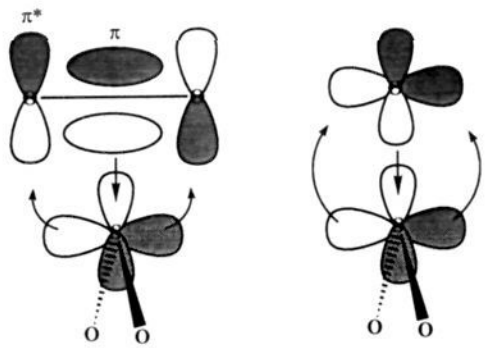

Figure 5. Illustration of the similarity in the donor/acceptor properties of O_2 and O interacting with a SO_2 fragment. In O_2 the π and π^* orbitals play the role of the two p orbitals of oxygen.

(**1**). Not only does this value represent the S–O bond strength in the SOO three-membered ring, it may also represent either the transition state or high-energy intermediate on the pathway to the decomposition products, SO_2 and O_2. With respect to the biradical (**3**), the S–O bond energy is –28.7 kcal/mol. Thus, breaking the second S–O bond is an exothermic process. An overall activation of about 18 kcal/mol would be consistent with a thermal stability of SO_4 to about 100–150 K.

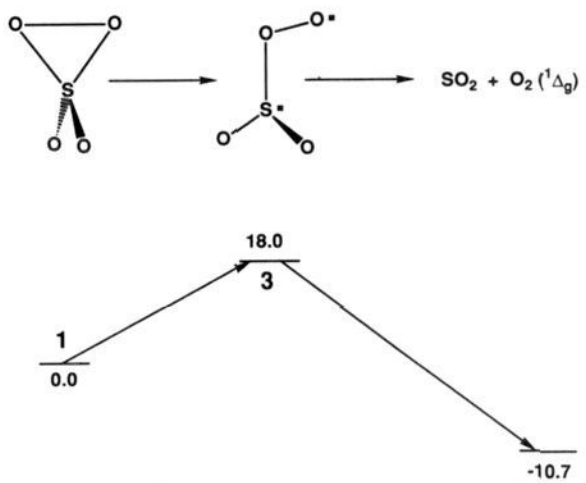

Figure 6. Possible SO_4 decomposition pathway to SO_2 plus O_2 through a peroxy-like transition state/intermediate (**3**). Calculated values are in kcal/mol relative to **1** at the MP4/6-31+G*//6-31+G* level. It is known that SO_4 is stable in a matrix to 100–150 K.

S_2O_3. A natural extension of this work is to determine the lowest energy species resulting from the removal of two electrons from thiosulfate to form disulfur trioxide, S_2O_3. In analogy with the results on SO_4, two alternatives were considered: one structure which contained an SSO three-membered ring (**11**) and one which contained an SOO three-membered ring and a terminal S–S bond (**12**). At the MP4/6-31+G*//6-31+G* level of theory, the structure with the SSO three-membered ring (**11**) is 45.8 kcal/mol more stable than the structure with a SOO three-membered ring (**12**). With respect to a sulfur atom in the ^1D state plus SO_3, the SSO ring structure (**11**) is predicted to be exothermic by 41.1 kcal/mol while the SOO ring structure (**12**) is predicted to be endothermic by 4.7 kcal/mol. The decomposition products are predicted to be SO_2 plus SO ($^1\Delta$), which is 20.6 kcal/mol exothermic with respect to **11**, rather than S_2O plus O_2 ($^1\Delta_g$), which is endothermic by 37.4 kcal/mol. The ground state of SO is the $^3\Sigma$ state which is predicted to be 16.6 kcal/mol lower in energy than the $^1\Delta$ state at the MP4/6-31+G* level.

The calculated structures **11** and **12**, which are given in Figure 1, are closely related to the C_{2v} SO_4 structure (**1**) with a sulfur atom replacing the oxygen atom of the ring (**11**) or at a terminal position (**12**). Why is there a strong preference for sulfur to be in the three-membered ring? One explanation is that a sulfur atom in a three-membered ring with two σ bonds (**11**) is expected to be preferable to a terminal sulfur atom with partial π bond character (**12**) due to the known preference for third-row elements to form σ rather than π bonds.

Vibrational frequencies and intensities have been calculated for both disulfur trioxide structures at the HF/6-31+G* level (Table VII). The symmetric and asymmetric SO_2 stretch (1320, 1509 cm^{-1}, respectively, HF/6-31+G*) should be diagnostic for the presence of **11**. Both stretches are relatively intense as is a ring mode at 715 cm^{-1}. Applying a 0.9 scaling factor, bands are predicted at 1358, 1188, and 644 cm^{-1}. As an indication that the

Table VII. Calculated Vibrational Frequencies (cm^{-1}) and IR Intensities (km/mol) at the HF/6-31+G* Level for **11** and **12**

	$O_2\overline{SSO}$ (**11**)				$SO\overline{SOO}$ (**12**)		
	HF/3-21G*	HF/6-31+G*	description		HF/3-21G*	HF/6-31+G*	description
a′	1331(315)	1320(345)	SO_2 s stretch	a′	1446(236)	1147(282)	SO stretch
	972(31)	975(52)	SSO ring		1171(148)	1152(192)	SOO ring
	698(156)	715(189)	SSO ring		837(242)	831(199)	SOO ring
	601(48)	601(24)	SSO ring		648(43)	626(72)	SS stretch
	527(35)	523(27)	scissor		484(29)	477(20)	bend
	420(5)	430(8)	bend		352(8)	346(4)	scissor
a″	1524(249)	1509(296)	SO_2 as stretch	a″	699(0)	759(7)	SSO as stretch
	485(32)	478(26)	bend		458(27)	453(21)	bend
	287(0)	282(0)	twist		307(2)	304(0)	twist

calculated frequencies of S_2O_3 are reliable, the calculated frequencies for S_2O (434, 781, 1352 cm^{-1}, HF/6-31+G*, unscaled) are in good agreement with experiment[35] (388, 679, 1165 cm^{-1}).

Conclusion

From the study of SO_4 species, it can be concluded that the species observed in an irradiated low-temperature matrix of SO_3 and O_3 is a SO_4 structure of C_{2v} symmetry containing a three-membered SOO ring. The ring structure is calculated to be lowest in energy and the vibrational frequencies and isotope shifts are in good agreement with experiment. A peroxy-like species, calculated to be 18.0 kcal/mol less stable, is a possible species on the decomposition path to SO_2 and O_2.

The most stable disulfur trioxide species, S_2O_3, is predicted to have two terminal oxygen atoms and a three-membered SSO ring. The structure is exothermic with respect to SO_3 plus a $S(^1D)$ atom which suggests that a possible route for the synthesis of this novel compound might be to generate singlet sulfur atoms in the presence of SO_3 in a low-temperature matrix. The vibrational frequencies are reported in the hopes that they will aid in the experimental identification of this molecule.

Acknowledgment. I thank the donors of the Petroleum Research Fund, administered by the American Chemical Society, for financial support. Computer time for this study was made available by the Alabama Supercomputer Network and the NSF-supported Pittsburgh Supercomputer Center. Dr. David Stanbury is acknowledged for many helpful discussions.